

PAPER • OPEN ACCESS

On possible reasons of positive near-anode voltage drop in high-current vacuum arc

To cite this article: D L Shmelev *et al* 2019 *J. Phys.: Conf. Ser.* **1393** 012026

View the [article online](#) for updates and enhancements.

Recent citations

- [Particle modeling of vacuum arc discharges](#)
Wei Yang *et al*



IOP | ebooks™

Bringing together innovative digital publishing with leading authors from the global scientific community.

Start exploring the collection—download the first chapter of every title for free.

On possible reasons of positive near-anode voltage drop in high-current vacuum arc

D L Shmelev^{1,2}, S A Barengolts³, M M Tsventoukh⁴, I V Uimanov¹ and L Wang⁵

¹ Institute of Electrophysics UD RAS, Amundsen Str., Yekaterinburg, 620016, Russia

² Ural Federal University, 19 Mira Str., Ekaterinburg, 620002, Russia

³ Prokhorov General Physics Institute RAS, 38 Vavilov Str., Moscow, 119991, Russia

⁴ P.N. Lebedev Physical Institute RAS, 53 Leninskii Ave., Moscow, 119991, Russia

⁵ Xi'an Jiaotong University, 28 Xianning West Road, Xi'an, 710049, China

E-mail: shmelev@iep.uran.ru

Abstract. In this paper we consider some reasons for the occurrence of a positive near-anode potential drop during current constriction in high-current vacuum arc. It is shown that if the radius of constriction is much larger than the electron mean free path, then a positive voltage drop in the near-anode plasma sheath does not occur, but an additional drop may occur in the near-anode plasma layer due to the anomalous resistance. If the current constriction radius is much less than the electron mean free path, then a positive voltage drop in the sheath arises under the usual condition, and the kinetic instabilities in the near-anode plasma do not develop.

1. Introduction

There are experimental evidences that under certain conditions a positive anode voltage drop occurs in the near-cathode region of the high-current vacuum arc (HCVA) [1], although the exact location of the potential drop is not determined experimentally. Some researchers believe that this positive voltage drop occurs inside the near-anode plasma sheath [1, 2], when an anode current density surpasses the electron thermal current density [3, 4]. Moreover, they suggest that this positive voltage drop may be the reason of the anode spot appearance.

However, in [5, 6] it is shown that for the plasma parameters typical for HCVA the anode voltage drop inside the anode plasma sheath remains negative even at a current density higher than the electron thermal current density. The reason for that is the formation in the near-anode plasma of the electron shifted Maxwell distributions with the velocity shift corresponding to the electron current velocity. At this condition the anode plasma sheath voltage drop remains negative at any current. Despite this conclusion the positive near-anode voltage drop formation is still possible. It does not have to be a voltage drop in the sheath. A geometric-ohmic voltage drop in the thin near-anode plasma layer aroused due to current constriction is also possible. In this paper, MHD and kinetic approaches have been used to study various possible scenarios for the formation of the positive voltage drop both in the anode plasma sheath and in the near-anode plasma region of HCVA. In particular, it was demonstrated the formation of the positive voltage drop in the anode plasma sheath when the radius of current constriction become less than the electron coulomb collision mean free path.



2. Near-anode voltage drop in 1D Cartesian model

To study the near-anode voltage drop in HCVA, special kinetic one-dimensional models using particle-in-cell (PIC) and Monte Carlo (MC) methods were developed [4].

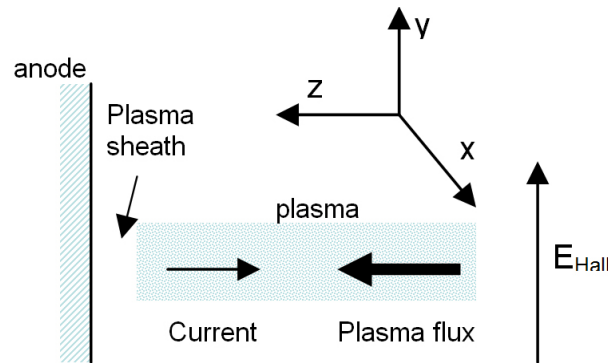


Figure 1. Geometry of the model.

The first model is one-dimensional in “flat” Cartesian geometry. Current density through the plasma cloud with the parameters typical for HCVA was specified in the model in order to get an electric potential distribution in the plasma and in the plasma sheath. The geometry of the problem is shown in figure 1.

The voltage drop in the plasma shell was calculated both with the application of an external oblique magnetic field and without the magnetic field. The results for plasma density in the range 10^{14} – 10^{15} cm $^{-3}$ (other parameters in table 1) are shown in figures 2–3. The figures show the dependence of dimensionless electron drift velocity at the sheath boundary V_0/V_{th} , $V_{th} = (8T_e/\pi m_e)^{0.5}$ on dimensionless sheath voltage drop ($e\phi/T_e$). Traditionally, it is assumed that the maximum drift velocity of electrons at the plasma boundary is $0.25V_{th}$, and the density of the electron current is equal to the density of the thermal electron current. The curve that corresponds with this behavior is curve-1 in figures 1–2. In fact, this is true only if electron distribution function (EDF) is close to the non-shifted Maxwell distribution function. In the case of one-dimensional current carrying plasma, the EDF is close to Maxwell distribution function shifted by the value of the current velocity of the electrons. For such a case, an approximate formula was obtained [5] (figure 2, curve 3). According to this formula, there is no restriction on the drift velocity of electrons at the plasma boundary, and the anode drop is always negative.

Table 1. Plasma parameters.

#	n_e (cm $^{-3}$)	Z	L (μ m)	T_e (eV)	T_i (eV)
4	10^{14}	1	100	4	1
5	10^{15}	1	100	4	1
6	10^{14}	1	100	4	1 no CC
7	10^{15}	1	33	4	1
8	10^{15}	2	33	4	1
9	10^{15}	1	33	4	12

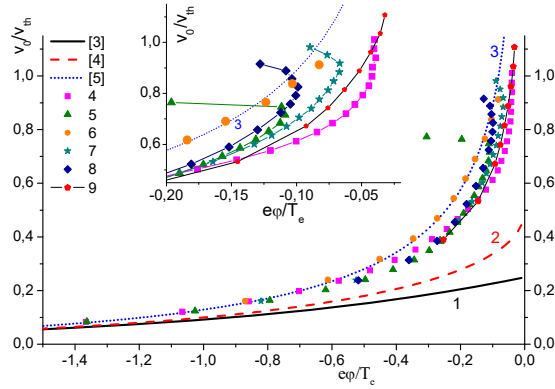


Figure 2. Electron velocity at sheath boundary as function of sheath potential drop. Plasma parameters correspondent to curves 4–9 are written in table 1.

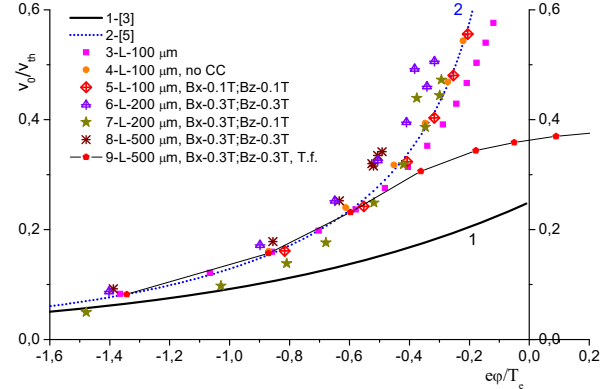


Figure 3. Electron velocity vs. voltage drop for plasma with oblique magnetic field. Parameters for curves 3–9 are shown in the figure.

In our calculations, the anode voltage drop also remained negative. The best similarity with the formula [5] was obtained for case 6 (table 1), in which Coulomb scattering was not considered. When V_0/V_{th} was approached to unity, the ion-sound and then Benemann instabilities developed in the plasma, which led to additional heating of electrons. In figure 2, the development of a strong instability is noted by a change in the slope of the curve. The negative anode drop, which had previously decreased in absolute value, begins to increase in absolute value with increasing V_0/V_{th} . If the criterion for the development of a strong instability is not satisfied, then the voltage drop monotonically decreases (figure 1, curves 4 and 9). For this case, an interpolation formula for the dependence of potential fall on electron drift velocity was obtained for use as boundary conditions in two-dimensional MHD and hybrid models [6].

$$\frac{e\phi}{T_e} = \text{Ln} \left[f \left(\frac{V_0}{V_{th}} \right) \cdot \frac{V_0}{V_{th}} \right], \quad (1)$$

$$f(x) = \min(4.0 - 0.444x^3 + 1.88x^2 - 3.14x + 2.891 + 0.04/x).$$

Let us consider how this situation can be affected by an external magnetic field directed at a certain angle to the anode (figure 3). This configuration of the magnetic field occurs in HCVA with an external axial magnetic field as a result of a combination of self and external magnetic fields. In this example, the plasma ion density is 10^{14} cm^{-3} , the ion charge state is 2. The range of magnetic fields (external and self) $\sim 0.1\text{--}0.3 \text{ T}$ is characteristic of HCVA. Only electrons are magnetized.

For the presence of normal electron conductivity in this case, the Hall electric field $E_{\text{Hall}} = [J \times B] \cdot (e \cdot c \cdot n_e)^{-1}$ is necessary (see figure 1). The Hall field must be set artificially. There is arbitrariness in the assignment of the spatial distribution of the field along Z . The fact is that on the anode the Hall field must be zero, but in plasma this field is nonzero. It is not connected with the near-anode plasma sheath. The Hall field exists in the plasma within the framework of quasi-neutrality. Thus, we assume the simplest dependence: Hall field falls linearly to zero, starting at $0.5 \text{ }\mu\text{m}$ from the anode. The external magnetic field in the problem can have x and z components (figure 1).

Anode fall in the case of an oblique magnetic field, as in the absence of a magnetic field, always remains negative (figure 3). An exception is curve 9. Curve 9 – the plasma parameters are the same as in the case of line 8, namely: $L = 500 \text{ }\mu\text{m}$, $B_x = B_z = 0.3 \text{ T}$. However, the voltage drop is measured over

the entire span of 500 μm , i.e. sheath drop plus drop on plasma. It is seen that the total voltage drop at high currents becomes positive. The drop on the layer remains negative (curve 8). The voltage drop in the plasma mainly occurs due to the anomalous resistance with developed modified ion-acoustic turbulence. That is, if someone tries to experimentally measure near-anode drop in such a case, then the voltage drop will be positive. But this is not due to a drop in the sheath (which remains negative), but because of anomalous ohmic drop in the plasma caused by ion-acoustic turbulence.

Qualitatively, the behavior of the anode potential drop in the presence of a magnetic field coincides with that in the absence of a field (compare figures 2 and 3). The voltage drop remains negative at current densities significantly higher than the density of the electron thermal current. The reason for this is that EDF in this model is practically a shifted Maxwell distribution function. But such a distribution function is formed if the characteristic length of the change in current density is much greater than the mean free path of electrons. In the considered examples, this criterion is satisfied.

3. Current constriction near anode due to Hall effect

Some researchers suggest that the positive drop in anode plasma sheath is the reason of some kind of instability, which leads to current constriction and the following anode spot formation [1, 2]. However, according to our opinion, the positive anode plasma sheath drop can appear as a result of near-anode current constriction, which in turn is caused by Hall effect [7–10].

To illustrate the current constriction in the HCVA, we consider the model problem of stationary current distribution in an axially symmetric interelectrode gap filled with plasma (geometry [8]). Taking into account the electron temperature, the system in the MHD approximation is described by the following equations [8]:

$$\frac{\partial B_0}{\partial t} + \frac{\partial u_{ez} B_0}{\partial z} + \frac{\partial u_{er} B_0}{\partial r} = \frac{c^2}{4\pi} \left(\frac{\partial}{\partial r} \left(\frac{1}{r\sigma} \frac{\partial r B_0}{\partial r} \right) + \frac{\partial}{\partial z} \left(\frac{1}{\sigma} \frac{\partial B_0}{\partial z} \right) \right), \quad \vec{J} = \frac{c}{4\pi} \nabla \times \vec{B}, \quad (2)$$

$$\frac{3}{2} n_e \left(\frac{\partial T_e}{\partial t} + \vec{u}_e \nabla T_e \right) + P_e \vec{\nabla} \vec{u}_e + \vec{\nabla} \chi \vec{\nabla} T_e = \frac{\vec{J}^2}{\sigma} - \frac{3m_e}{\tau_{ei}} (T_e - T_i) \quad (3)$$

The surface of the electrode is equipotential. Therefore, (2) has a non-trivial anode boundary condition:

$$\frac{J_r}{\sigma} - \frac{1}{en_e c} J_z B_0 + \frac{1}{c} u_{iz} B_0 - \frac{1}{en_e} \frac{\partial P_e}{\partial r} = \frac{\partial \varphi_a}{\partial r} \quad (4)$$

where the anode voltage drop (φ_a) is obtained from (1). With the plasma parameters typical for HCVA, the second term on the left-hand side (4) leads to an anode current constriction (Hall effect).

Let us consider this effect on the example of a gap (radius 2.75 cm, distance between electrodes 1 cm, current 10 kA, $z = 2$) filled with plasma with fixed densities $6 \times 10^{14} \text{ cm}^{-3}$ and $4.75 \times 10^{14} \text{ cm}^{-3}$ and initial temperature 3 eV. It is seen (figure 4) that the Hall effect leads to a strong constriction of the current at the anode, and the lower the plasma density, the stronger the constriction. For $n = 4.75 \times 10^{14} \text{ cm}^{-3}$, the current density in the center of the anode is more than three times the electron thermal current. In this case, the voltage drop in the near-anode sheath remains negative in accordance with the expression (1) obtained from kinetic modeling (figure 5). The heat flux density in the center of the anode is about of $2.7 \times 10^5 \text{ W} \cdot \text{cm}^{-2}$. At this heat flux, the surface temperature of the copper anode in one millisecond will reach the boiling point, after which the anode spot should occur [11]. That is, with this approach, the occurrence of the anode spot can be explained without the appearance of the positive anode voltage drop. However, as can be seen from figure 4, the radius of the current constriction is rather small. In this example, it is on the order of several millimeters. In this case, the electron-ion collisions length can be estimated as $\sim 0.2 \text{ mm}$, which is significantly less than the radius of contraction. Thus, the shifted EDF has time to form and the use of (1) is justified.

However, with a further decrease in plasma density and maintaining the current density, the characteristic scale of the current constriction may become smaller than the electron collision length.

In this case, approximation (1) is not applicable and a positive voltage drop in the sheath may occur. Such conditions can occur in the case of triggered HCVA and in discharges with a small anode [12].

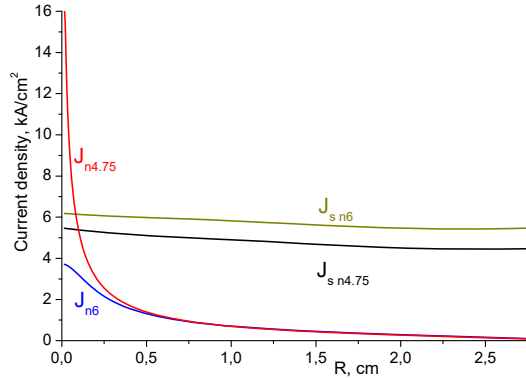


Figure 4. Densities of electron thermal current (J_s) and normal component of electron current (J) on anode side for two plasma densities $6 \cdot 10^{14} \text{ cm}^{-3}$ and $4.75 \cdot 10^{14} \text{ cm}^{-3}$.

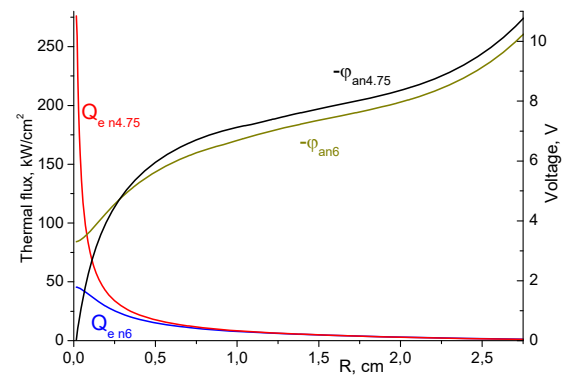


Figure 5. Electron thermal flux from plasma to anode (Q_e) and voltage drop in anode sheath (ϕ_a) for two plasma densities $6 \cdot 10^{14} \text{ cm}^{-3}$ and $4.75 \cdot 10^{14} \text{ cm}^{-3}$.

4. Near-anode voltage drop in 1D spherically symmetric model

Let us consider the case when the radius of the current is shorter than the electron mean free path and the shifted EDF has not possibility to be formed. For this purpose, a one-dimensional kinetic model of near-anode plasma with a spherical cone geometry was constructed.

Let us consider an example with an internal boundary with a radius of $r_0 = 20 \text{ }\mu\text{m}$, the external boundary with $r_1 = 120 \text{ }\mu\text{m}$, plasma density $n = 10^{14} \text{ cm}^{-3}$, $T_e = 3 \text{ eV}$. The electron current is set on the outer boundary r_1 , and a space charge layer is appeared on the inner side, which is necessary for the current to pass. Due to the selected geometry, the current density at the internal boundary is greater than the current density at the external boundary by factor of $(r_1/r_0)^2$. The collision length for this plasma is about 2 mm, which is much larger than the size of the model system. In this case, the EDF on the inner boundary differs substantially from shifted Maxwell EDF (figure 6). If at the inner boundary $V_e > 0.25V_{th}$, then a positive potential drop occurs in the near-electrode layer (figure 7). As can be seen from figures 7–8, when a positive anode voltage drop occurs, the electric field of the sheath squeezes the plasma from the electrode until the electric field pressure equals the total plasma pressure, and the current density at the sheath boundary approaches the thermal current density. Subsequently, the sheath oscillates at a frequency of the order of the ion plasma frequency. An electron beam is formed in the gap that appears. In this case, the kinetic current instabilities in the plasma do not develop.

Thus, in this model of spherical current constriction at the anode, when the condition $V_e > 0.25V_{th}$ is satisfied, in the near-anode sheath a positive drop in electric potential occurs. The occurrence of a positive potential drop is accompanied by an increase in heat flow to the anode. As can be seen from figure 9, for model plasma with a density of 10^{14} cm^{-3} , the heat flux may exceed $10^5 \text{ W}\cdot\text{cm}^{-2}$. This is sufficient to achieve the boiling point on the anode surface during a time about of 1 ms and the appearance of the anode spot [8, 11]. The heat flux and the potential drop make aperiodic oscillations with a frequency of the order of the ion plasma frequency. When an anode spot appears in an HCVA, the voltage drop across the arc increases and the voltage oscillation amplitude increases [11], which, in principle, correlates with the behavior of these quantities in our calculations for $V_e > 0.25V_{th}$. Note that as the radius of the current constriction increases to values exceeding the electron mean free path, the threshold electron velocity of the onset of a positive fall gradually increases.

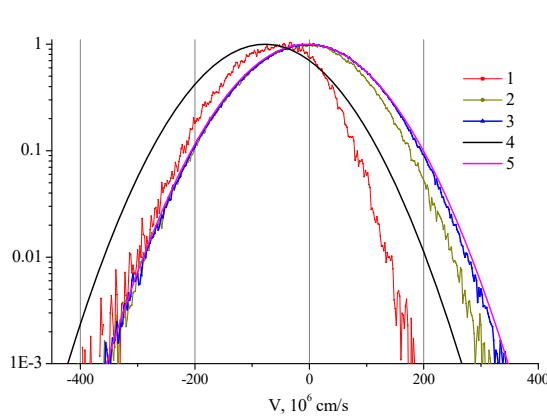


Figure 6. EDF in different points of calculation domain. Curves 1, 2, 3 – are calculated EDF at 15, 50, 100 μm from anode. Curves 4, 5 – are shifted Maxwell EDF at 15, 100 μm from anode calculated using average electron temperature and drift velocities. Current density at r_1 is $2 \text{ kA}\cdot\text{cm}^{-2}$.

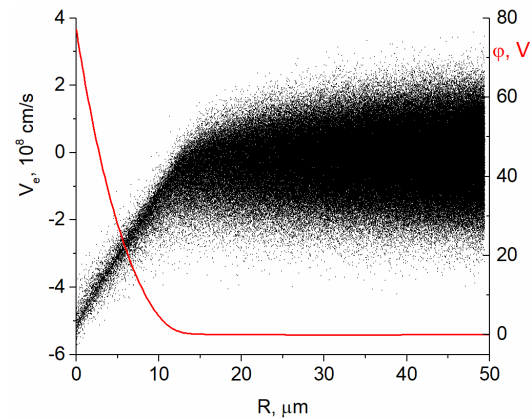


Figure 7. Phase portrait of electrons (black dots) and the distribution of electric potential (red curve). The current density at the internal boundary is $\sim 2 \text{ kA}\cdot\text{cm}^{-2}$. Internal (anode border) at $R = 0$.

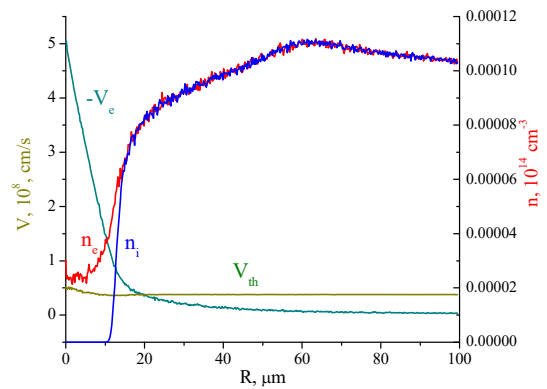


Figure 8. Electron drift velocities, electron and ion densities in the model gap. Current density at r_1 is $2 \text{ kA}\cdot\text{cm}^{-2}$.

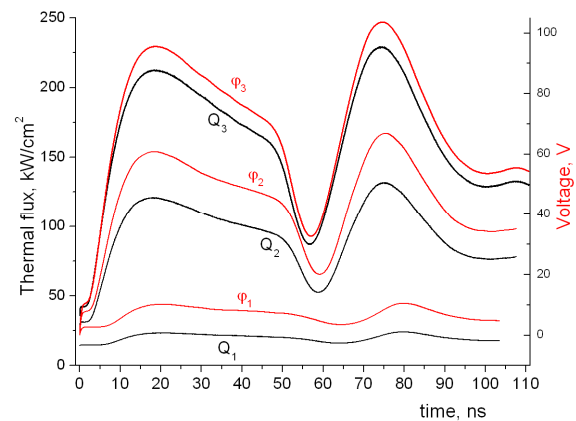


Figure 9. Electron heat flux to the anode (Q) and potential drop at the calculated interval (ϕ) as function of time. Current densities at r_1 are: 1) $\sim 1 \text{ kA}\cdot\text{cm}^{-2}$ ($\sim 2 \cdot J_{th}$); 2) $\sim 1.67 \text{ kA}\cdot\text{cm}^{-2}$; 3) $\sim 2 \text{ kA}\cdot\text{cm}^{-2}$ ($\sim 4 \cdot J_{th}$).

It should be noted that after the anode is heated and the onset of intense evaporation, an additional plasma arises at the anode and the conditions for the existence of a positive voltage drop and Hall current constriction (4) are violated. Thus, these mechanisms cannot ensure the maintenance of high heat flux to the anode in the mode of a developed anode spot. Recall that in the case of strong evaporation from the anode, a positive potential drop in the near-anode sheath may again occur due to pushing the plasma away from the anode by a stream of evaporated atoms [13].

5. Conclusion

In our work, we once again reminded that the near-anode current constriction in HCVA due to the Hall effect can provide heat flux, which is sufficient for the appearance of the anode spot.

In the case of sufficiently dense plasma, when the radius of the current constriction at the anode is much larger than the electron mean free path, the formation of the near-anode sheath was modeled within the one-dimensional PIC-DSMC approximation. It was shown that in this case the near-anode voltage drop remains negative at any current density. It was shown that oblique magnetic field has little effect on the formation of near-anode voltage drop. However, an additional positive potential drop may occur in the near-anode region (not in the sheath) due to the anomalous resistance.

In the case of sufficiently rarefied plasma, when the radius of the current at the anode is less than the electron mean free path, the formation of the near-anode sheath was modeled within the one-dimensional spherically symmetric PIC-DSMC model. It is shown that in this case, if the condition $V_e > 0.25V_{th}$ is fulfilled, a positive voltage drop in the near-anode sheath occurs. The occurrence of a positive potential drop is accompanied by an increase in heat flux to the anode. Heat flux and potential drop make aperiodic oscillations with a frequency of the order of ion plasma frequency.

Acknowledgments

This work was supported in part by RFBR (grant Nos. 17-02-00346, 18-08-00547, 19-08-00783, 19-58-53006), by RAS Program (project No. 11) and UB RAS Program (project No. 18-2-2-16), as well as by National Natural Science Foundation of China (project No. 51911530113).

References

- [1] Dyuzhev G A, Lyubimov G A and Shkol'nik S M 1983 *IEEE Trans. Plasma Sci.* **PS-11** 36
- [2] Nemchinskii V A 1983 *Sov. Phys.-Tech. Phys.* **28** 146
- [3] Tonks L and Langmuir I 1929 *Phys. Rev.* **34** 876
- [4] Boxman R L and Goldsmith S 1983 *J. Appl. Phys.* **54** 592
- [5] Londer Ya I and Ulyanov K N 2013 *Plasma Phys. Rep.* **39** 849
- [6] Shmelev D L, Barengolts S A and Tsventoukh M M 2014 *Plasma Sources Sci. Technol.* **23** 062004
- [7] Wieckert C A and Egli W 1989 *IEEE Trans. Plasma Sci.* **17** 649
- [8] Schade E and Shmelev D L 2003 *IEEE Trans. Plasma Sci.* **31** 890
- [9] Wang L, Qian Z, Huang X, Jia S and Shi Z 2013 *IEEE Trans. Plasma Sci.* **41** 2015
- [10] Shmelev D L and Uimanov I V 2015 *IEEE Trans. Plasma Sci.* **43** 2261
- [11] Schade E 2005 *IEEE Trans. Plasma Sci.* **33** 384
- [12] Scheiner B, Baalrud S D, Yee B T, Hopkins M M and Barnat E V 2015 *Phys. Plasmas* **22** 123520
- [13] Shmelev D L 2013 *IEEE Trans. Plasma Sci.* **41** 1969